Mid-IR Interband Cascade Lasers

Rui Q. Yang, Cory J. Hill, Yueming Qiu
Jet Propulsion Laboratory, California Institute of Technology, Pasadena, California

ABSTRACT

Efficient mid-IR interband cascade (IC) lasers are developed based on III-V semiconductor materials to cover wavelength range from 2.7 to 5.6 μm. These IC lasers reuse injected electrons in cascade stages for photon generation with high quantum efficiency to achieve high output powers. Also, IC lasers have low threshold current density with very efficient use of applied voltage, resulting in reduced power consumptions. Single-mode distributed feedback lasers have been made, and integrated into aircraft and balloon instrument which made measurements of CH_4 and HCl. In this work, the characteristics of IC lasers and their recent development are reviewed.

INTRODUCTION

Compact and reliable mid-infrared sources are needed for many applications such as gas sensing, environmental monitoring, medical diagnostics, free space communications, infrared countermeasures (IRCM), chemical warfare monitoring and IR lidar. The availability of efficient mid-IR semiconductor diode lasers will enable sensitive detection of many gases such as CH_4, C_2H_2, HC_3N, CO, CO_2, HCl, C_2H_6, and H_2CO, and their isotopes, of great interest in atmospheric and planetary science. Requirements for such lasers include a relatively high output power and continuous wave (cw) operation either at ambient temperature or at temperatures accessible with thermoelectric (TE) coolers.

Antimonide-based mid-IR interband cascade (IC) lasers [1], which reuse injected electrons in cascade stages for photon emission (Fig. 1), can have high quantum efficiency and low threshold current density with efficient use of applied voltage. These IC lasers can have a wide wavelength tailoring range, well covering important 3-5 μm spectral region. Theoretical calculations [2, 3] projected the feasibility of mid-IR IC lasers to operate in continuous wave (cw) mode up to room temperature with high output power. These mid-IR lasers are promising in meeting requirements of many above mentioned applications. Since the proposal of type-II IC lasers in 1994 [1], significant progress has been achieved toward developing high-performance mid-IR IC lasers [4-14]. For applications in chemical sensing, distributed feedback (DFB) IC lasers [8] have been demonstrated stable single-mode operation in cw mode for the wavelength range from ~3.2 to 3.5 μm. These DFB IC lasers have been employed for the detection of gases [14] such as methane (CH_4), hydrogen chloride (HCl), and formaldehyde (H_2CO) [15]. IC lasers have been flown on aircraft and high-altitude balloon instruments and measured CH4 and HCl profiles in the stratosphere. In this paper, we will review the characteristics of IC lasers and their recent development.

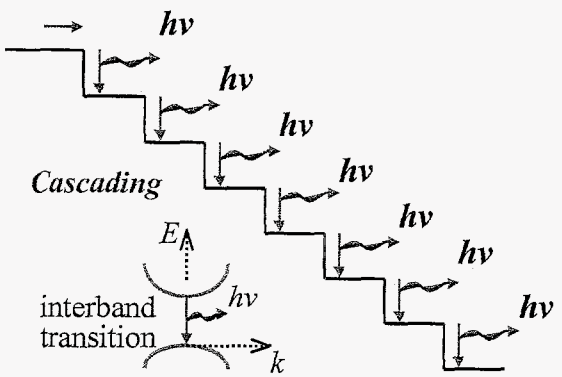

Fig. 1 Illustration of the interband cascade laser

CHARACTERISTICS OF MID-IR INTERBAND CASCADE LASERS

The Sb-based IC laser structures are composed of multiple coupled quantum wells (QWs) made from Al(In)Sb, InAs, and Ga(In)Sb III-V compound semiconductor materials and have cascade stages ranging from 8 to 35 covering emission wavelength range from ~2.7 to 5.7 μm [6-14]. IC laser wafers were grown on GaSb or GaAs substrates in a solid source Gen-III molecular beam epitaxy (MBE) system. The wafers were usually processed into deep-etched mesa-stripe lasers with metal contacts on the top layer and the bottom substrate. Laser bars were typically cleaved to form cavities of 0.5 to 1.5 mm long with both facets left uncoated. The laser bars were affixed with indium or silver epoxy, epilayer side up, onto a copper heat-sink and were then

Table 1. Characteristics of some representative interband cascade lasers

Wafer	N_C	W (μm)	λ (μm) at 80 K	J_{th} 80K (A/cm^2)	V_{th} (V) at 80K	λ (μm) at T_{max} cw/pulse	T_{max} (K) cw/pulse	J_{th} (A/cm^2) at T_{max} cw/pulse	V_{th} (V) at T_{max} cw/pulse
J430	12	20	2.86	28	5.89	3.07/3.19	208/325	689/1510 (300K)	6.28/7.93 (300K)
J375X	12	15	3.08	27	5.22	3.225/3.31	212/325	702/1911 (300K)	5.88/8.55 (300K)
		15	---			3.233/---	217/--	715/---	5.98/---
J377X	12	15	3.15	17	5.1	3.3/3.37	212/325	640/1960 (300K)	6.1/8.22 (300K)
J578	12	20	3.2	31	5.63	3.401/3.491	213/325	533/1347 (300K)	6.69/9.36 (300K)
J730	12	15	3.27	14	4.82	3.5/3.55	230/320	613/1366 (300K)	5.25/6.1 (300K)
J732	12	20	3.05	41.7	5.367	3.27/3.36	210/340	517/1226 (300K)	5.71/6.75 (300K)
		15	3.03	15.6	5.333	3.3/3.38	237/350	622/1080 (300K)	5.87/6.59 (300K)
		150	3.06	9.3	5.27	3.22/3.36	172/320	142/630 (300K)	5.41/8.06 (300K)
J738	12	15	3.12	15	5.06	3.37/3.45	235/350	622/1111 (300K)	5.56/6.67 (300K)
J768	12	15	3.28	19	4.61	3.55/3.6	228/340	622/1342 (300K)	5.02/5.58 (300K)
J655	12	15	3.21	19	5.39	3.45/3.528	223/325	667/1563 (300K)	6.24/8 (300K)
J653	12	15	3.25	16	4.94	3.46/3.52	219/325	604/1671(300K)	5.57/7.06 (300K)
J657	12	15	3.25	18	5.276	3.44/3.5	206/300	700/2040	5.83/9
J134	15	150	3.02	12	7.1	3.13/3.28	165/325	162/1051 (300K)	7.44/10.2 (300K)
J137	15	110	3.11	8.9	6.82	3.245/---	175/315	206/1209 (300K)	7.23/10.5 (300K)
		30	3.12	10.3	6.8	3.265/3.34	200/310	293/---	7.41/---
J439	15	15	3.38	17	5.87	3.615/---	212/300	475/2307	6.82/11.8
J173	18	110	3.22	14.8	7.9	3.38/3.47	165/270	136/712	8.38/12.69
		50	---			3.435/---	175/---	220/---	8.29/---
		30	3.24	29	7.3	3.436/3.53	190/310	410/1700 (300K)	8.01/9.6 (300K)
J366X	18	15	3.41	40	7.01	3.63/3.71	195/290	438/4910	7.3/---
J241	18	30	3.5	11	7.32	3.64/---	180/---	193/---	8.68/---
J330X	18	15	3.687	25	6.61	3.791/3.78	175/280	340/5000	7.085/11.6
J165X	23	150	3.67	8	8.8	3.825/4.11	150/300	126/2440	9.28/16.7
J165Y	23	150	3.66	10	8.82	3.782/4.09	135/300	76/2020	8.99/16.1
J243	28	150	4.31	30	9	4.46/4.7	110/237	146/1151	9.48/14
		20	---			4.563/4.7	125/240	457/2575	9.4/13.7
		20	4.36	110	9.31	4.65/---	145/---	433/-----	9.68/---
J435X	30	15	5.09	43	8.04	5.45/5.7	165/260	470/2240	8.66/13.21
J381X	35	15	5.12	35	9.3	5.44/5.6	163/240	380/1060	10.5/12.8

mounted on the temperature-controlled cold finger of an optical cryostat. A thermopile power meter was used to calibrate the cooled InSb detector used in our measurements and to measure the optical output in cw mode. It should be noted that the power measurements reported below are conservative: only a 10% loss from the transmission through the optical cryostat window was assumed without accounting for beam divergence and other factors. The emission spectra were obtained by focusing the output beam onto the entrance slit of a 0.55-m monochromator or a Fourier Transform infrared (FTIR) spectrometer. In pulsed mode, current pulses of 1-μs duration and 1 kHz repetition rate were injected into all laser devices at various temperatures. Some performance characteristics of representative lasers are summarized in Table 1 in order of increasing cascade stages N_C and lasing wavelength λ near their thresholds.

From table 1, one can see that most IC lasers have threshold current density J_{th} range from only 8 to a few tens of A/cm^2 at 80 K with threshold voltage V_{th} from ~5 to 9 V depending on lasing wavelength and the number of cascade stages. This translates to low power consumptions (~30 mW) for narrow (15 μm-wide) mesa lasers to operate with threshold currents of a few mA at 80 K. At higher temperatures, threshold currents increase and are in the range from a few tens of mA to above 200mA depending on device size. For almost all devices, their output powers are higher than 10 mW in cw mode at low temperatures and can still deliver 1 mW even at relatively high temperatures (e.g. 200 K for some relatively narrow stripe lasers), sufficient for in-situ gas sensing applications. For broad-area lasers, output power greater than 100 mW can be routinely achieved at temperatures above 77 K. Detailed characteristics of some devices are discussed below.

Broad-area IC lasers with high output powers

With large emission facet, a single broad-area laser can deliver high output power. As shown in Fig. 2, a 150-μm-wide and 1-mm-long mesa stripe laser made from wafer J732 delivered cw optical output power ~290 mW/facet at ~84 K and 700 mA at which the heat-sink temperature was brought up to about 84 K from 80 K due to significant heating and limited cooling power of liquid N_2 in the measurement dewar. This device lased in cw mode at temperatures up to 177 K near 3.22 μm, with threshold current density J_{th} from 11 A/cm^2 at 80 K to ~175 A/cm^2 at 177 K. The power efficiency is as high as 18.2% at 80 K, which is very good for mid-IR diode lasers. The slope efficiency near the threshold is about 611, 533, 424, 300, 202 mW/A at 80, 110, 140, 160, 170 K, corresponding to differential external quantum efficiency of ~300%, 265%, 214%, 153%, 104%, respectively, which exceed the conventional limit of unity due to the cascade process. The high quantum efficiency can significantly improve signal to noise ratio when modulated for some

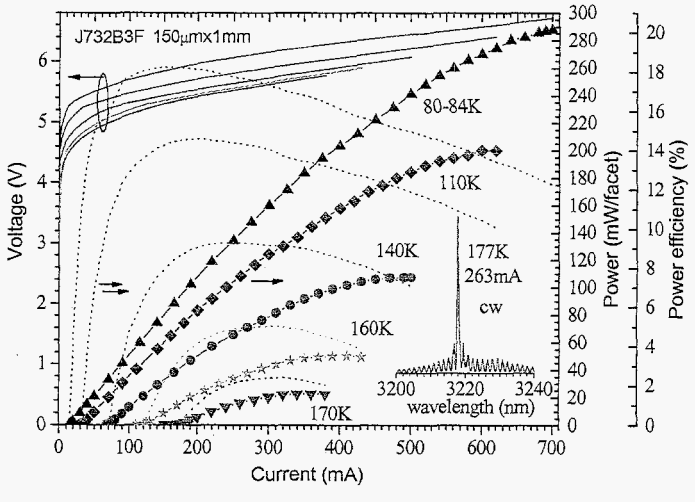

Fig. 2 Current-voltage-light characteristics and power efficiency (dotted) of a mesa-stripe laser. The inset shows the lasing spectrum of the laser operating at 177 K and 263mA.

system applications. The decrease of quantum efficiency with temperature and current is attributed mainly to heating effect. This device exhibited a large specific thermal resistance R_{sth} (~46 Kcm^2/kW at 177 K, due in part to imperfect mounting to the Cu-heat-sink), which ultimately limits the highest cw operating temperature and attainable output power. In pulsed mode, this broad-area device lased at temperatures up to 320 K near 3.36 μm as shown in Fig. 3, with low threshold current density (e.g. 684A/cm^2 at 300K).

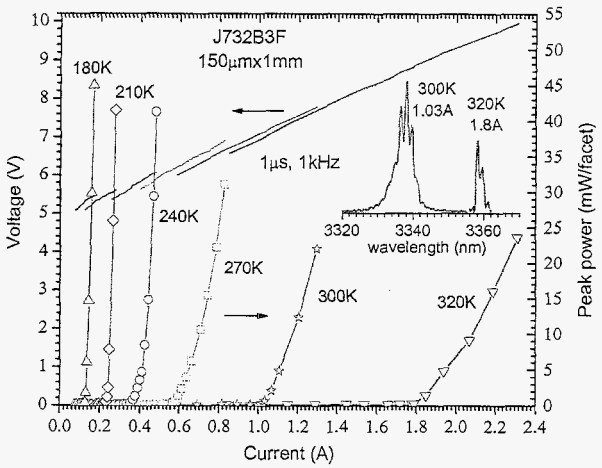

Fig. 3 *I*-V-*L* characteristics of a mesa-stripe laser in pulsed mode. The inset shows the lasing spectra of the laser operating at 300 K and 320K.

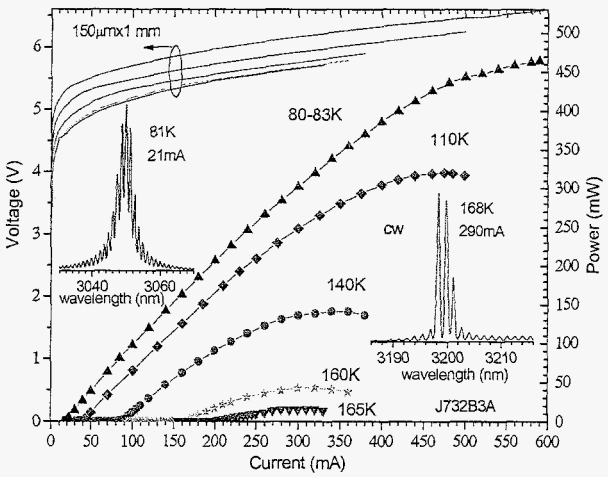

Fig. 4 *I*-V-*L* characteristics of a mesa laser with HR(~78%)/AR(~5%) coating. The inset shows the lasing spectra of the laser at 81 K and 168K.

The high power IC lasers can have useful applications in remote sensing and may be used with reflectance spectroscopy to search for H_2O on the Moon. To obtain higher powers, facet coating and better thermal management can be applied to IC lasers. Fig. 4 showed the characteristics of a broad-area (150μmx1mm) IC laser (made from the same wafer J732) operating in cw mode from 80 to 165 K. With high reflection (HR) coating (~78%) on the back facet and an antireflection (AR) coating (~5%) on the front facet, more than 460 mW was obtained from the front facet of this laser at 83 K with a current of 590 mA, even though the specific thermal resistance is still large (R_{sth}~41 Kcm^2/kW at 168 K). Further higher output powers can be achieved with an array of lasers or/and epi-layer-side-down mounting, opening up more possibilities of applications requiring powers in the watts or higher levels.

Narrow mesa stripe lasers for high temperature operation

For achieving cw operation at high temperatures, wafers are processed into narrow (15-20 μm) mesa stripe devices so that total current required for lasing is reduced with less heat. Without any special treatment such as epilayer-side-down mounting or electroplating thick Au layer on the top, a 15-μm-wide mesa stripe IC laser made from wafer J732 was able to lase in cw mode at temperatures up to 237 K [15]. Fig. 5 shows characteristics of another 15-μm-wide mesa stripe IC laser made from wafer J738, which lased in cw mode at temperatures up to 235 K near 3.375 μm. At the threshold, the differential resistance exhibited an abrupt decrease, indicative of a significant change of carrier transport when the device began lasing. The threshold current is only a few mA at low temperatures and is less than 140 mA even at 235 K

with a threshold voltage near 5.5 V. The light output powers are greater than 1 mW at temperatures above 200 K, sufficient for in situ gas sensing. This implies that the laser can be operated in cw mode with commercially available thermoelectric (TE) coolers for some applications. Although 200 K is accessible with commercial multi-stage TE coolers, the operation at this temperature is still inconvenient and a TE cooler may consume significant power (>10W) to reach such a temperature. Operation in cw mode at higher temperatures (≥280K) or room temperature is more desirable.

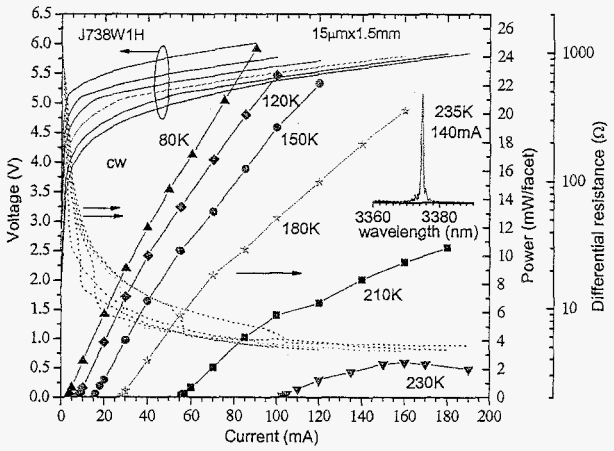

Fig. 5 *I*-V-*L* characteristics and differential resistence (dotted) of a 15-μm-wide mesa-stripe laser. The inset shows the lasing spectrum of the laser operating at 235 K and 140mA.

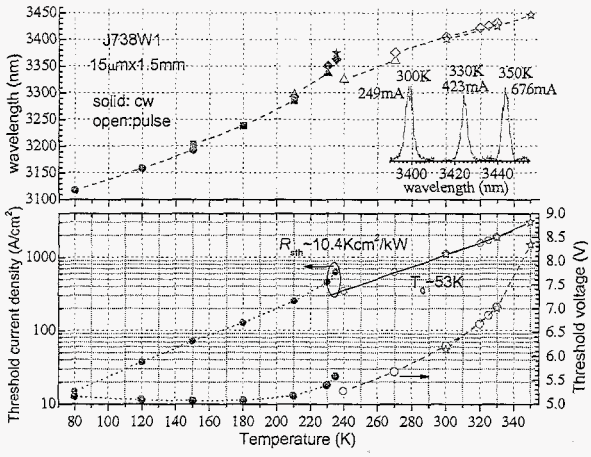

Fig. 6 Threshold properties (bottom) and lasing wavelengths (top) near thresholds for 15-μm-wide mesa-stripe lasers made from J738. The inset shows lasing spectra of a laser operating at 300,330,350 K.

The main issue that currently limits IC lasers operating in cw mode at room temperature is the thermal transport, rather than any inherent constraints [14]. This can be elaborated by examining characteristics of the laser under pulsed conditions with negligible heating. Fig. 6 shows threshold properties of the laser and the lasing wavelength near threshold under cw and pulsed conditions in a wide temperature range. The laser can operate in pulsed mode at temperatures up to 350 K (near 3.445 μm), well above the maximum cw operating temperature (235 K). The lasing wavelength increases more rapidly in cw operation at higher temperatures due to more heating with higher threshold current. While in pulsed mode, the lasing wavelength increases at an approximately linear rate $d\lambda/dT$~1 nm/K with the temperature as the band-gaps of constituent III-V semiconductor materials decrease with the temperature. By comparing the difference in temperature between a pulsed and cw mode operation with equal threshold current, the specific thermal resistance is estimated to be 10.4 K·cm^2/kW at 235 K. This value of R_{sth} for narrow mesa stripe IC lasers is significantly lowered compared to broad-area IC lasers, but is considerably higher than the values reported for narrow-stripe intraband quantum cascade lasers (~2-2.4 K · cm^2/kW epi-side-up [16], ~0.33-0.9 K · cm^2/kW epi-side-down [17]) and for epi-side-down mounted broad-area type-II QW mid-IR lasers (≤2 K · cm^2/kW for optical pumping [18]). If the specific thermal resistance of IC lasers could be reduced to 2-3 K · cm^2/kW by improving thermal management such as putting a thick electroplated Au layer on the top of the device, cw operating temperature of IC lasers would be raised up to 290-310 K based on the threshold characteristics shown in Fig. 6.

INTERBAND CASCADE LASERS ON GaAs SUBSTRATES

Interband cascade laser structures have been grown on lattice mismatched GaAs substrates [20] and devices made from IC laser wafers on GaAs have exhibited cw operation and room temperature pulsed operation [12]. Since GaAs substrate has a refractive index lower than that of cascade region, it can naturally serve as part of bottom optical cladding layer such that the light leakage into the substrate as in case of lasers on GaSb substrate is greatly reduced. Fig. 7 shows current-voltage-light (*I*-V-*L*) characteristics of a 12-stage 20-μm-wide and 1.5-mm-long mesa-stripe laser made from wafer J580Sn which was grown on an *n*-type GaAs substrate. Also shown in Fig. 7 is *I*-V-*L* characteristics of 20-μm-wide and 1.5-mm-long mesa-stripe laser made from wafer J578, which was grown on an *n*-type GaSb substrate and has the nominally same cascade structure as J580Sn. The laser on GaAs substrate lased in cw mode at temperatures up to 182 K with emission wavelength near 3.3 μm (inset of Fig. 7) despite of significantly high threshold voltage (~8.3-9.6 V) due mainly to a large series resistance from the *n*-type GaAs substarte to the *p*-type GaSb buffer layer. It is noticeable that the output power of the laser on GaAs at 80 and 120 K is substantially higher than that of the laser on GaSb substrate. This suggests that the laser on GaSb substrate, which has about 3 μm thick InAs/AlSb superlattice bottom cladding layer, has a substantial light leakage into the substrate with possible more optical loss or/and less effective light collection from the GaSb substrate, even though the laser on GaSb lased in cw at temperatures up to 213 K near 3.4 μm. The laser on GaAs substrate lased in pulsed mode at temperatures up to 305 K near 3.39 μm. Nevertheless, the laser on GaAs substrate has significantly high threshold current as shown in Fig. 8 because the material quality on GaAs substrate is inferior to that of the laser on GaSb substrate. With efforts to improve material quality and appropriate band structure engineering for reducing threshold current and voltage, IC lasers on GaAs or other lattice-mismatched substrates may become viable for certain applications in future.

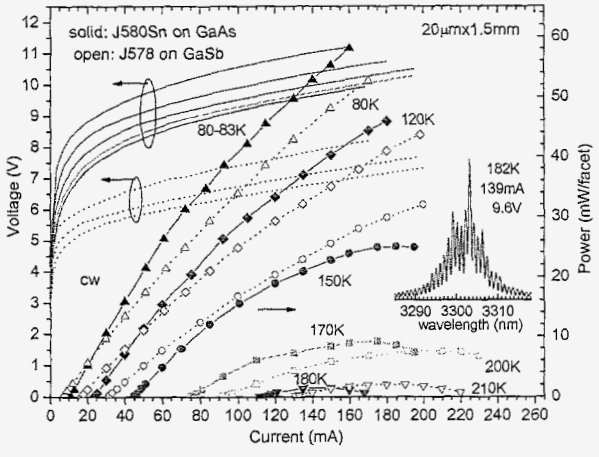

Fig. 7 *I*-V-*L* characteristics of 20-μm-wide mesa-stripe lasers on GaAs and GaSb substrates. The inset shows the lasing spectrum of the laser on GaAs at 182 K and 139mA.

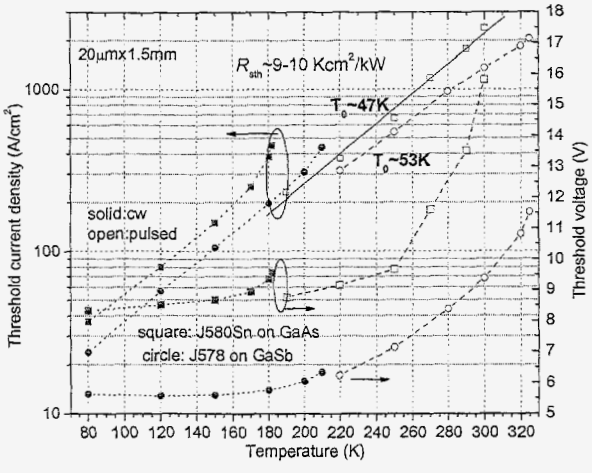

Fig. 8 Threshold properties for 20-μm-wide mesa-stripe lasers on GaAs (squares) and on GaSb (circles) substrates.

DISTRIBUTED FEEDBACK INTERBAND CASCADE LASERS

Distributed feedback (DFB) IC lasers with stable single-mode output in cw mode have been demonstrated for the wavelength range from ~3.2 to 3.6 μm. These DFB IC lasers have been employed for the detection of gases such as formaldehyde (H_2CO) [15], methane (CH_4) and hydrogen chloride (HCl) [12].

Distributed feedback IC lasers are made with DFB gratings on the top of the wafers patterned by e-beam lithography. The wavelength of a DFB mode from the laser is essentially determined by the grating period Λ according to $\lambda=2n_{eff}\Lambda$, where n_{eff} is the temperature-dependent effective index of the laser waveguide. Fig. 9 shows lasing spectra of two DFB IC lasers (J439D3E and J439D3F) with different grating periods. At 80 K, each of the two DFB lasers exhibited a dominant DFB mode at 3406.2 and 3412.6 nm, respective, with the side-mode suppression ratio greater than 40 dB at a current of 6 mA. The stop-band due to DFB grating is clearly shown by a below-threshold emission spectrum at a current of 3 mA for the device J439D3E and has a width of ~3.5 nm, indicative of index-coupled DFB lasers [19]. When the temperature is raised to 100 K, the effective index increases slightly, which red shifts the DFB mode to ~3416.2 nm from 3412.6 nm as shown in the top part of Fig. 9 for device J439D3F. The temperature tuning rate of wavelength $d\lambda/dT$ is about 0.18nm/K. The increase of current also slightly red shifts the DFB mode since the resulting heat raises the device temperature, but at a smaller pace especially at low temperatures with low current injection.

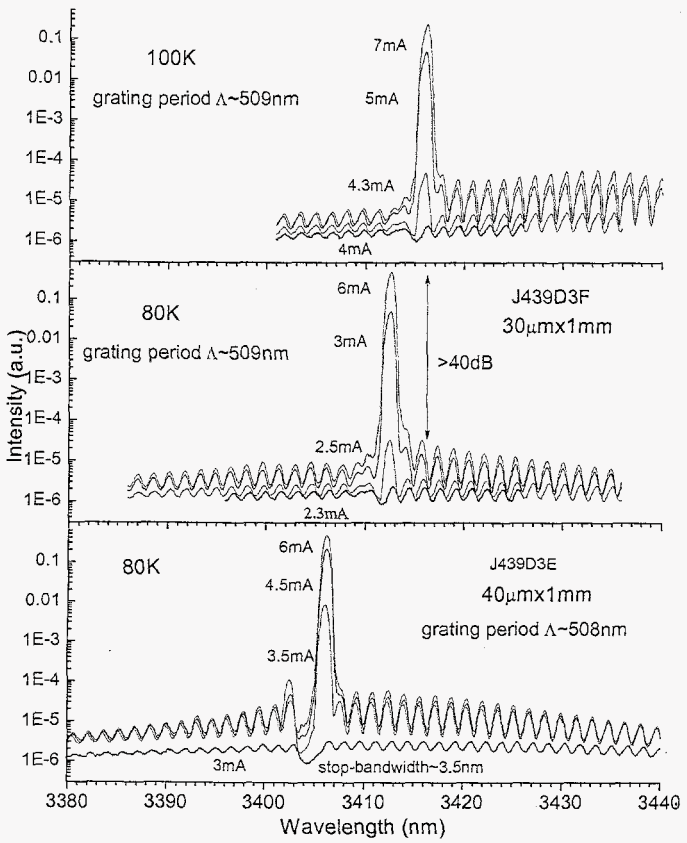

Fig. 9 Lasing spectra for two DFB lasers made from wafer J439.

Fig. 10 shows near threshold lasing spectra and tuning curve of a DFB IC laser (made from J738) operated at relatively high temperatures. The laser exhibited a stable single-mode emission which can be tuned over 10 nm in a temperature range from 170 to 215 K. The temperature tuning rate of the wavelength $d\lambda/dT$ is about 0.28nm/K, larger than the value for DFB lasers at low temperatures due to substantial heating with significantly increased current injection required to the device at higher temperatures.

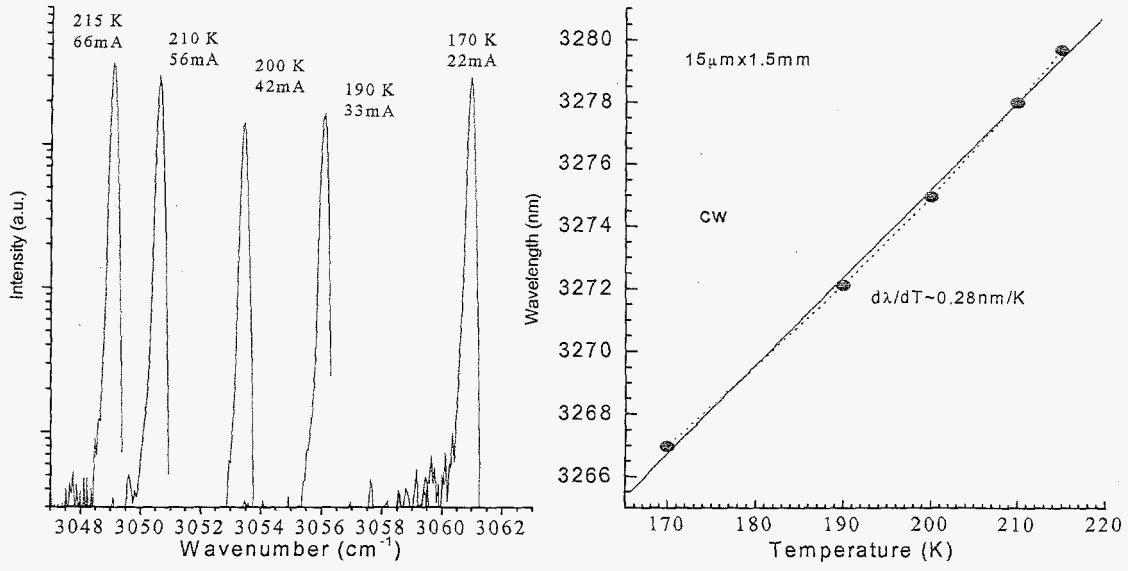

Fig. 10 Near threshold lasing spectra (left) and wavelengths (right) of a DFB laser (made from wafer J738) at several temperatures.

SUMMARY

Significant progress in the development of efficienct mid-IR IC lasers has recently been made in terms of high output powers (e.g. >460 mW at 80 K), low threshold current densities (e.g. ~630 A/cm^2 at 300 K), and high temperature operation (e.g. 350 K in pulsed and 237 K in cw modes). DFB IC lasers have been developed with stable single-mode emission and can be tuned over 10 nm in a relatively wide range of temperature. These DFB lasers have been employed for gas detection and have been integrated into aircraft and balloon instrument which made measurements of CH_4 and HCl. These accomplishments were achieved even though device fabrication and packaging were in a preliminary stage with relatively large specific thermal resistance and are still being perfected. The main objective remains to achieve cw operation at room temperature for meeting the requirements of many practical applications. However, when contrasted with other semiconductor laser technologies such as InP- and GaAs-based QC lasers, the amount of effort expended in developing Sb-based IC lasers has been very limited. Still, there is significant room for improvement considering that many parameters in device design and MBE growth have not been optimized, as well as in device fabrication and packaging. Specifically, the mesa stripes of the lasers described here could be reduced further and a thick gold layer could be deposited on top and sides of the device to remove heat more efficiently, resulting in cw operation at significantly higher temperatures. Various options in device design, material growth, fabrication and packaging will be explored in our future effort.

ACKNOWLEDGMENTS

The authors gratefully acknowledge R. E. Muller and P. M. Echternach for e-beam writing of DFB gratings, Baohua Yang and Archcom Technology, Inc. for laser device processing, and C. M. Wong and J. Li for testing of some lasers. They are grateful to S. Forouhar, P. J. Grunthaner, S. D. Gunapala, D. L. Jan, E. A. Kolawa, T. N. Krabach, and C. F. Ruoff for their support. The

research described in this paper was performed at the Jet Propulsion Laboratory (JPL), California Institute of Technology, and was supported in part by the National Aeronautics and Space Administration (NASA), Advanced Environmental Monitoring and Control Technology Development Program, Enabling Concepts & Technologies Program, and JPL internal Research & Technology Development program.

REFERENCES

1. R. Q. Yang, at *7th Inter. Conf. on Superlattices, Microstructures and Microdevices*, Banff, Canada, Aug. 1994; Superlattices and Microstructures **17**, 77 (1995).
2. J. R. Meyer, I. Vurgaftman, R. Q. Yang, and L. R. Ram-Mohan, Electronics Letters, **32**, 45 (1996).
3. I. Vurgaftman, J. R. Meyer, and L. R. Ram-Mohan, IEEE Photo. Tech. Lett. **9**, 170 (1997).
4. R. Q. Yang, Microelectronics J. **30**, 1043 (1999); and references therein.
5. R. Q. Yang, *et al.*, IEEE J. Quantum Electron. **38**, 559 (2002); and reference therein.
6. R. Q. Yang, C. J. Hill, B. Yang, J. K. Liu, Appl. Phys. Lett. **83**, 2109 (2003).
7. C. J. Hill, B. Yang, R. Q. Yang, Physica E **20**, 486 (2004).
8. R. Q. Yang, C. J. Hill, B. Yang, C. M. Wong, R. Muller and P. Echternach, Appl. Phys. Lett. **84**, 3699 (2004).
9. J. L. Bradshaw, *et al.*, Physica E **20**, 479 (2004).
10. R. Q. Yang, C. J. Hill, B. Yang, C. M. Wong, IEEE Photon. Technol. Lett. **16**, 987 (2004).
11. C. J. Hill, C. M. Wong, B. Yang, R. Q. Yang, Electronics Lett. **40**, 878 (2004).
12. R. Q. Yang, C. J. Hill, L. E. Christensen, C. R. Webster, Proc. SPIE **5624**, 413 (2005).
13. C. J. Hill, and R. Q. Yang, J. Crystal Growth **278**, 167 (2005).
14. R. Q. Yang, C. J. Hill, B. Yang, Appl. Phys. Lett. **87**, 151109 (2005).
15. M. Horstjann, *et al.*, Appl. Phys. B **79**, 799(2004).
16. J. Faist, F. Capasso, C. Sirtori, D. L. Sivco, A. L. Hutchinson, A. Y. Cho, Appl. Phys. Lett. **67**, 3057 (1995).
17. C. Gmachl, A. M. Sergent, A. Tredicucci, F. Capasso, A. L. Hutchinson, D. L. Sivco, J. N. Baillargeon, S. N. G. Chu, and A. Y. Cho, IEEE Photo. Technol. Lett. **11**, 1369 (1999).
18. W. W. Bewley, C. L. Felix, E. H. Aifer, D. W. Stokes, I. Vurgaftman, L. J. Olafsen, J. R. Meyer, M. J. Yang, and H. Lee, IEEE Quantum Electron. **35**, 1597 (1999).
19. H. Kogelnik and C. V. Shank, J. Appl. Phys. **43**, 2327 (1972).
20. C. J. Hill, and R. Q. Yang, Appl. Phys. Lett. **85**, 3014 (2004).